

1 **Auto-Immunoproteomics Analysis of COVID-19 ICU Patients Revealed Increased Levels of**
2 **Autoantibodies Related to Male Reproductive System**

3
4 Frank Schmidt^{1*#}, Houari B. Abdesselem^{2,11#}, Karsten Suhre³, Muhammad U. Sohail¹, Maryam
5 Al-Nesf^{4,5}, Ilham Bensmail², Fathima Mashod¹, Hina Sarwath¹, Joerg Bernhardt⁶, Ti-Myen
6 Tan^{7,8,9}, Priscilla E Morris^{7,8,9}, Edward J. Schenck¹⁰, David Price¹⁰, Nishant N. Vaikath¹¹, Vidya
7 Mohamed-Ali^{5,12}, Mohammed Al-Maadheed^{5,12}, Abdelilah Arredouani¹³, Julie Decock¹⁴, Jonathan
8 M. Blackburn^{7,8,9}, Augustine M.K. Choi¹⁰, Omar M. El-Agnaf^{11*}

9
10 ¹Proteomics Core, Weill Cornell Medicine - Qatar, Doha, Qatar.

11 ²Proteomics Core Facility, Qatar Biomedical Research Institute (QBRI), Hamad Bin Khalifa University
12 (HBKU), Qatar Foundation, Doha, Qatar.

13 ³Bioinformatics Core, Weill Cornell Medicine - Qatar, Doha, Qatar.

14 ⁴Hamad General Hospital, Hamad Medical Corporation, Doha, Qatar.

15 ⁵Center of Metabolism and Inflammation, Division of Medicine, Royal Free Campus, University College
16 London, Rowland Hill Road, London NW3 2PF, UK.

23 ⁶Institute for Microbiology, University of Greifswald, Greifswald, Germany.

24 ⁷Department of Integrative Biomedical Sciences, Faculty of Health Sciences, University of Cape Town,
25 South Africa.

26 ⁸Sengenics Corporation, Level M, Plaza Zurich, Damansara Heights, Kuala Lumpur 50490, Malaysia.

27 ⁹Institute of Infectious Disease and Molecular Medicine, Faculty of Health Sciences, University of Cape
28 Town, South Africa.

29 ¹⁰Department of Medicine, Division of Pulmonary and Critical Care Medicine, New York Presbyterian
30 Hospital – Weill Cornell Medical Center, Weill Cornell Medicine, New York, NY, USA.

31 ¹¹Neurological Disorders Research Center, QBRI, HBKU, Qatar Foundation, Doha, Qatar.

32 ¹²Anti-Doping Laboratory Qatar, Doha, Qatar.

33 ¹³Diabetes Research Center, QBRI, HBKU, Qatar Foundation, Doha, Qatar.

34 ¹⁴Cancer Research Center, QBRI, HBKU, Qatar Foundation, Doha, Qatar.

35
36 # These authors contributed equally to the work.

37
38 * Corresponding Authors:

39
40 Frank Schmidt
41 Address: Proteomics Core, Weill Cornell Medicine - Qatar, Doha, Qatar
42 Tel: 0097450446815, E-Mail: frs4001@qatar-med.cornell.edu

43
44 Omar El-Agnaf
45 Address: Neurological Disorders Research Center, QBRI, HBKU, Qatar Foundation, Doha,
46 Qatar.
47 Tel: 0097455935568, E-Mail: oelagnaf@hbku.edu.qa

48
49 Conflict of Interest Disclosures: no conflict of interest

50

51 Running Head: KREX-autoimmune COVID-19 replication study
52
53 Manuscript word count: 4871 words
54 Number of Figures: 9
55 Number of Supplemental Tables: 1, Number of Supplemental data file: 1
56

57 **Abstract**

58 The role of autoantibodies in coronavirus disease (COVID-19) complications is not yet fully
59 understood. The current investigation screened two independent cohorts of 97 COVID-19 patients
60 (Discovery (Disc) cohort from Qatar (n = 49) and Replication (Rep) cohort from New York (n =
61 48)) utilizing high-throughput KoRectly Expressed (KREX) immunome protein-array technology.
62 Autoantibody responses to 57 proteins were significantly altered in the COVID-19 Disc cohort
63 compared to healthy controls ($P \leq 0.05$). The Rep cohort had altered autoantibody responses
64 against 26 proteins compared to non-COVID-19 ICU patients that served as controls. Both cohorts
65 showed substantial similarities ($r^2 = 0.73$) and exhibited higher autoantibodies responses to
66 numerous transcription factors, immunomodulatory proteins, and human disease markers.
67 Analysis of the combined cohorts revealed elevated autoantibody responses against SPANXN4,
68 STK25, ATF4, PRKD2, and CHMP3 proteins in COVID-19 patients. KREX analysis of the
69 specific IgG autoantibody responses indicates that the targeted host proteins are supposedly
70 increased in COVID-19 patients. The autoantigen-autoantibody response was cross-validated for
71 SPANXN4 and STK25 proteins using Uniprot BLASTP and sequence alignment tools. SPANXN4
72 is essential for spermiogenesis and male fertility, which may predict a potential role for this protein
73 in COVID-19 associated male reproductive tract complications and warrants further research.

74

75 **Keywords:** COVID-19, Autoantibodies, Immunoproteomics, SPANXN4, STK25, and Male
76 reproductive system

77 **Significance Statement**

78 Coronavirus disease (COVID-19), caused by the SARS-CoV-2 virus, has emerged as a global
79 pandemic with a high morbidity rate and multiorgan complications. It is observed that the host
80 immune system contributes to the varied responses to COVID-19 pathogenesis. Autoantibodies,
81 immune system proteins that mistakenly target the body's own tissue, may underlie some of this
82 variation. We screened total IgG autoantibody responses against 1,318 human proteins in two
83 COVID-19 patient cohorts. We observed several novel markers in COVID-19 patients that are
84 associated with male fertility, such as sperm protein SPANXN4, STK25, and the apoptotic factor
85 ATF4. Particularly, elevated levels of autoantibodies against the testicular tissue-specific protein
86 SPANXN4 offer significant evidence of anticipating the protein role in COVID-19 associated male
87 reproductive complications.

88

89 **Introduction**

90 Coronavirus disease (COVID-19), caused by novel SARS-CoV-2 virus, has emerged as global
91 pandemic with severe complications and high morbidity rate. The disease manifests a wide range
92 of clinical symptoms, which are exacerbated by overactive and malfunctioning immune system of
93 the host. Despite extensive research on innate and adaptive immune responses in COVID-19, little
94 is known about the role of autoantibodies on disease progression and severe complications.

95 Infection with the SARS-CoV-2 causes a variety of symptoms, with most cases being moderate or
96 asymptomatic, and only a smaller proportion advancing to more severe state of COVID-19
97 disease¹. Many questions about the COVID-19 pathophysiology remain open, particularly why
98 some people develop severe disease symptoms while others remain asymptomatic.

99 Acute respiratory distress syndrome (ARDS) affects a small percentage of patients, whereas others
100 experience persistent lung damage and multi-organ illness that lasts months, even after the virus
101 has been eliminated from the body². High expression of angiotensin-converting enzyme 2 (ACE2)
102 receptors in several organs of the body extends infection beyond respiratory tract, resulting in
103 complex multiorgan complications³. ACE2 receptors are highly expressed in the male reproductive
104 system, demonstrating the involvement of SARS-CoV-2 in male fertility, which is one of the
105 unexplained manifestations of COVID-19⁴.

106 Autoantibodies have been identified in significant proportion of COVID-19 hospitalized patients
107 with positive correlation with immune responses to SARS-CoV-2 proteins⁵. Several studies
108 observed significant rise in a diverse range of autoantibodies against immunomodulatory proteins,
109 α - and ω -interferons, cardiolipin and prothrombin during antiviral responses in severely ill
110 COVID-19 patients^{6, 7, 8, 9, 10, 11}. Particularly, autoantibodies against immune-related signaling
111 proteins were found to contribute to COVID-19 pathogenesis by antagonizing the function of the
112 innate immune system¹². Although there have been some reports on disease-modifying
113 autoantibody responses, the immunological and clinical consequences of autoantibodies in
114 COVID-19 are yet to be fully understood. Here, we therefore screened total IgG autoantibody
115 responses against 1,318 human proteins in COVID-19 patients using KREX immunome protein-
116 array technology. Sengenics KREX technology employs full-length, naturally folded proteins that
117 allow maximum epitopes binding to discover autoantibody biomarker proteins¹³. The quantitative
118 signal measured on the arrays for each autoantibody-autoantigen pair is directly proportional to
119 the autoantibody concentration in the blood with higher autoantibody titres to these proteins
120 simplistically implying higher autoantigen concentrations in COVID-19 patients compared to
121 controls, albeit the correlation is non-linear.

122 Autoantibody-based precision immuno-profiling has previously been shown to aid discovery of
123 biomarkers of immune-related adverse events, as well as therapeutic prediction of drug response¹⁴.
124 In the present study, by utilizing a broad array-based immunoproteomics strategy that
125 simultaneously quantifies autoantibody responses across multiple organ systems in ICU COVID-
126 19 patients and post recovery cohort, we aimed to better identify novel markers of comorbidities
127 in COVID-19 patients. We identified a number of novel markers in COVID-19 patients that are
128 also associated with male fertility, such as the sperm protein SPANXN4¹⁵, the androgenic kinase

129 STK25^{16, 17}, the apoptotic factor ATF4¹⁸, the calcium channel regulator protein kinase PRKD2¹⁹,
130 and the multivesicular protein CHMP3²⁰.

131

132

133 **Methods**

134 **Study design, samples collection and processing and ethics**

135 We used blood samples and clinical data of patients from two independent COVID-19 cohorts to
136 conduct a comprehenisve anlaysis of autoantibodies using novel KREX technology.

137 ***Discovery (Disc) cohort***

138 The Disc cohort included forty-nine COVID-19 patients from Qatar who were admitted to Hamad
139 Medical Corporation hospitals. All recruited patients had confirmed SARS-CoV-2 positive RT-
140 PCR results of sputum and throat swabs. All patients had severe COVID-19 disease (WHO
141 guideline)²¹ and were admitted to intensive care unit (ICU). Peripheral blood was collected within
142 five to seven days of admission and processed into plasma and serum, which were stored at -80°C,
143 until further analysis. Ethical approval for this cohort was obtained from the Hamad Medical
144 Corporation Institutional Review Board Research Ethics Committee (reference MRC-05-003), and
145 Qatar Biomedical Research Institute- Institutional Review Board (Reference QBRI-IRB 2020-06-
146 19).

147 ***Healthy controls***

148 Age and gender matched healthy volunteers (n=48) with no prior COVID-19 infection history and
149 with normal oxygen saturation and vital signs were used as controls. The Anti-Doping Laboratory-
150 Qatar recruited them for blood collection. Individuals with medical history or with cognitive
151 disabilities were excluded. All participants (patients and controls) provided written informed
152 consent prior to enrolment in the study.

153 ***Replication (Rep) cohort***

154 The replication cohort consisted of forty-eight adult patients who were admitted to the ICU of New
155 York-Presbyterian Hospital (NYP)/Weill Cornell Medical Center (WCMC) from March to April
156 2020. All patients were RT-PCR confirmed SARS-CoV-2 positive and displayed ARDS or
157 pneumonia symptoms. The cohort is part of the Weill Cornell Biobank of Critical Illness, a registry
158 which attempts to recruit and enroll all patients being admitted to WCMC ICU for clinical
159 investigations. The WCMC COVID Institutional Data Repository (COVID-IDR), a manually
160 abstracted registry of COVID-19 patients that was developed to record patient demographics and
161 allied health parameters. Laboratory parameters, ventilation records, respiratory variables and vital
162 signs were recorded and documented at Weill Cornell-Critical Care Database for Advanced
163 Research (WC-CEDAR)²². The processes for recruiting patients, collecting data, and processing
164 samples had all been previously documented^{23, 24}. Only patients that gave informed consent were
165 included. IRB approvals for this cohort were obtained from NYP/WCMC with reference number
166 20-05022072 and 1405015116.

167

168 **Non-COVID-19 ICU controls**

169 Twenty-eight patients admitted to NYP hospital ICU between 2014 to 2019 were included as non-
170 COVID-19 ICU controls for the Rep cohort. These patients were suffering from bacterial sepsis
171 ARDS (N = 15), influenza ARDS (N = 4), and influenza pneumonia (N = 9). The patient
172 recruitment, medical history, and sampling procedures for the non-COVID ICU control cohort are
173 the same as those described for the Rep cohort.

174 **Sengenics assay description and data pre-processing**

175 The Disc cohort samples were processed at Qatar Biomedical Research Institution (QBRI) for
176 KREX immunoproteomics. The Rep cohort samples were processed at the Sengenics facility in
177 Kuala Lumpur, Malaysia. Samples of Disc cohort and controls were analyzed for antigen-specific
178 autoantibodies using Immunome protein arrays (Sengenics), developed using KoRectly Expressed
179 (KREX) technology to provide a high-throughput immunoassay based on correctly folded, full
180 length and functional recombinant human proteins expressed in insect cells, thereby displaying a
181 full repertoire continuous and discontinuous epitopes for autoantibody binding^{25, 26}. The
182 Immunome arrays contain more than 1,600 human antigens, enriched for kinases, signaling
183 molecules, cytokines, interleukins, chemokines, as well as known autoimmune- and cancer
184 antigens. Plasma samples of Rep cohort and non-COVID-19 ICU control patients were then
185 processed for autoantibodies on a custom array containing a subset of 1,318 human proteins
186 (Sengenics).

187 Samples were viral-inactivated in 10% Triton X-100 for 2 hours at room temperature. Samples
188 were then diluted in Serum Albumin Buffer (SAB) at optimized dilution (50-fold dilution).
189 Microarray slides were prepared in four-well plates slide. Samples including controls were
190 randomized and applied to the microarray slides for 2 hours and samples' IgGs were then detected
191 by secondary Cy3-labeled IgG antibodies. Slides were scanned at a fixed gain setting using the
192 Agilent G4600AD fluorescence microarray scanner generating a 16-bit TIFF file. A visual quality
193 control check was conducted and any array showing spot merging or other artefacts were re-
194 assayed. A GAL (GenePix Array List) file containing information regarding the location and
195 identity of all probed spots was used to aid with image analysis. Automatic extraction and
196 quantification of each spot was performed using GenePix Pro 7 software (Molecular Devices)
197 yielding the median foreground and local background pixel intensities for each spot.

198 Biotinylated human IgG (detected by fluorescently labelled secondary antibody) and biotinylated
199 human anti-IgG (detected only when plasma or serum is added to the slide) were used as positive
200 controls to assess assay integrity. Extrapolated data was then filtered, normalized and transformed
201 as follows: Briefly, the median background pixel intensity (RFU) was subtracted from the median
202 foreground pixel intensity (RFU) for each antigen to give the median net intensity per spot (RFU);
203 CVs were calculated for each antigen based on the quadruplicate technical replica spots for each
204 antigen on a given array, any antigens with CV above 20% were flagged and outlier spots removed,
205 providing that at least two valid values remained; net intensity values for each antigen in a given
206 sample were calculated as the mean of the net intensity values for technical replica spots on that
207 array; and data was normalised across replica arrays based on the Cy3-BSA controls as previously

208 described²⁷. Z-scores were then calculated by subtracting the overall mean antigen intensity
209 (within a single sample) from the net intensity data for each antigen in that sample, and dividing
210 that result by the standard deviation of all of the measured net intensities in that sample, according
211 to the formula: $z = (x - \mu) / \sigma$ where x is the net intensity of an antigen in a given sample, μ is the
212 mean net intensity calculated across all antigens in that sample, and σ is the standard deviation of
213 the net intensities for all antigens in that sample. All downstream statistical analysis was done
214 based on the calculated z-scores.

215 **Sequence identity and antigen specificity analysis for selected proteins**

216 We needed to be cautious in directly comparing the results across different antigens on the arrays
217 because the autoantigen-autoantibody response is not always linear and is an indirect way of
218 prediction of protein concentrations. Since it can depend amongst others on both B cell activation
219 and sequence identity among proteins that express similar antigen epitopes. To check this latter
220 possibility, we selected two proteins (SPANXN4 and STK25) that showed the highest
221 autoantibody alterations to perform their sequence alignment and antigen specificity analysis.
222 Uniprot BLASTP program was used to compare proteins sequences. All human and viral protein
223 sequences with more than 50% sequence similarity were aligned for epitope mapping to determine
224 whether the evaluated RFU values were specific to the protein of interest or could be derived from
225 highly homologous epitopes on other proteins.

226 **Protein pathways prediction**

227 The assignment of KREX array proteins to functional KEGG categories and their hierarchical
228 organisation was displayed by using Paver, a software for the visualization of Voronoi Treemaps²⁸.
229 Any main category is displayed in different colors. The cell sizes were calculated according the
230 signal intensity of the proteins immunofluorescence (highly fluorescent signals give larger cells).
231 Functional Enrichment Analysis was performed to identify biological functions that were over-
232 represented in differentially expressed proteins with a p-value less than 0.05. Differentially
233 expressed proteins, both up-regulated and down-regulated, were used separately as proteins of
234 interest and the proteins detected from all probes were used as the background set. The proteins
235 were further annotated using KEGG- and WIKI-Pathways data prior to performing Fisher's exact
236 test to determine pathways in which the proteins of interest were significantly over-represented.
237 This analysis was performed on R 3.6.2 using clusterProfiler 3.14.3. GOSemSim was used to
238 eliminate redundant GO-BP results. Only significantly over-represented pathways with a p-value
239 less than 0.05 (-log10 p-value cut-off 1.3) are shown.

240 **Statistical analysis**

241 Proteins are reported using the symbols of the genes that encode them to offer a clear and uniform
242 nomenclature. Autoantibody response, measured as relative fluorescence units (RFU), was
243 normalized to calculate z-score. Statistical analysis was performed using R (version 4.1.0) and

244 rstudio (version 1.4.1717). Two kinds of inferal statistical tests were performed to test the
245 hypotheses of whether a given autoantibody was differentially expressed in COVID cases versus
246 controls. First, the means between cases and controls were compared using a linear model, using
247 the z-scored autoantibody responses as dependant variables and the COVID state as independent
248 variable (coded as 0=controls and 1=cases). Note that this approach is equivalent to conducting an
249 unrelated T-test and that the effect size of the linear model matches the estimated difference of the
250 means in a T-test. Second, binarized autoantibody responses were tested against cases versus
251 controls using Fisher's exact test. The cutoff for binarization of the autoimmune response was set
252 to one. As the response is z-scored, this means that all samples with an RFU score above one
253 standard deviation from the mean were considered as being positive for the respective
254 autoantibody whereas all other were considered negative. The Disc and Rep cohorts were analyzed
255 separelly and then merged. Therefore three sets of p-values were obtained for each of the
256 continous and binarized trait analyses.

257 Following comparisons were made:

258 • Differential autoantibody response analysis: COVID-19 cases versus controls for

259 ○ Forty-nine Disc COVID-19 patients vs. fourty-eight controls.

260 ○ Forty-eight Rep COVID-19 patients vs. twenty-eight non-COVID-19 ICU controls.

261 ○ Combined ninety-seven COVID-19 vs. seventy-six controls from both Disc and Rep
262 cohorts.

263 • Pearson's correlation analysis of fifteen Disc cohort patients sampled at the time of ICU
264 admission (T1) and six weeks follow-up (T2).

265 • Principal component analysis and pearson's correlation analysis to compare two cohorts.

266

267

268 **Results**

269 **Study design and cohort specific information**

270 In the present work, two ethnically independent cohorts of COVID-19 patients were evaluated for
271 their autoimmune response (total IgG-response) against 1,318 naturally folded human proteins
272 (antigens). The Disc cohort was recruited at ICU of HMC in Doha, Qatar and included 49 COVID-
273 19 cases and 48 healthy controls, majority of whom were male. A second cohort was recruited
274 from the ICU of NYP Hospital, USA, which included 48 COVID-19 cases and 28 control patients
275 and served as a Rep study. In addition, patients who were admitted to the NYP ICU and had
276 infectious diseases other than COVID-19, such as bacterial sepsis ARDS or H1N1 pneumonia,
277 were included as controls for the Rep cohort. Because of the special composition of the cohorts,
278 we were able to specifically look for COVID-19-related autoantibody signals compared with
279 healthy-baseline- and general infection-baseline-titres. A combined analysis (discovery and
280 replication) allowed stringent COVID-19-specific autoimmune responses to be monitored. Table
281 1 summarises the demographic and status-specific information of the study cohorts.

282 **General autoantibody response in healthy and COVID-19 patients**

283 To discover functional IgG-related autoantibodies that could influence COVID-19 predictions
284 and/or outcomes, we used the KREX high-throughput autoantibody assay technology that includes
285 a variety of known human-autoantigens such as cancer-, kinase-, interleukins-, cytokine,
286 ribonuclear transcription and signalling-proteins²⁹. Total IgG autoantibody responses were
287 quantified for 1,600 proteins in the Discovery Cohort and for a subset of 1,318 proteins in the
288 Replication Cohort. However, to increase stringency and reduce complexity, only the 1,318
289 overlapping proteins were subsequently used in the analysis pipeline. The majority of antigens on
290 the array are found in the cytoplasm, nucleus, or cell membrane, but there are also proteins from
291 the mitochondria, endoplasmic reticulum, and cytoskeleton.

292 The KREX assay reports RFU values for autoantigen-specific autoantibody binding, with linearity
293 over 6 orders of magnitude and with a detection limit in the pg/ml range. These measured RFU
294 values correlate directly with the antigen-specific IgG autoantibody titres, since ligand binding
295 theory shows that the measured signal on-array is linearly proportional to autoantibody
296 concentration. Thus, a higher RFU value for a specific autoantibody-autoantigen interaction
297 indicates a higher autoantibody titre, whilst a higher antibody titer in turn implies a higher
298 autoantigen concentration (or repeated exposure to the autoantigen), accepting that this latter
299 correlation is non-linear. In a first overview, the general intensity distributions were calculated
300 based on the mean autoantibody-antigen titers across all samples and further examined using
301 KEGG-Brite-based Voronoi treemaps using the replication cohort as an example (Figure 1).
302 Approximately 1,150 of the 1,318 proteins could be assigned to the annotation, with the relative
303 size of each cell on the Voronoi treemaps reflecting the observed autoantibody response against
304 that protein (Figure 1 left). Nearly all proteins showed a total IgG AB-signal in the cases and the
305 corresponding controls, the latter represents the natural autoimmunity or the healthy repertoire of
306 autoantibodies. In Figure 1 right, the corresponding pathways are summarized in different colors,

307 with most proteins belonging to the MAPK pathway (light blue), followed by transcription factors
308 (green), chromosomal proteins (green), ribosomes (all blue), and metabolic proteins (yellow). A
309 few proteins belong to the cell cycle (red), chemokines (cyan) or cancer (black). The 10 highest
310 autoantibody titers were found against RBPJ, TPM1, TACC1, KRT19, PTPN20, TBCB, KRT15,
311 AFF4, HSPD1, and CBFA2T3, many of these are structure related proteins. The 10 proteins with
312 the lowest titers were AIF1, IL18, NCK1, COMMD3, NEK11, TGFBR2, SLA, PKM, MAPK6,
313 and MLKL, many of which are cytoplasmic proteins involved in phosphorylation.

314 **Relative autoantibody response in the Disc cohort revealed significantly higher level of**
315 **SPANXN4 and ATF4**

316 To examine the effects of SARS-CoV-2 infection on the autoantibody response, we first performed
317 a differential expression analysis in Disc cohort between COVID-19 cases and healthy controls
318 using T-test. Autoantibody responses of fifty-seven proteins were altered significantly (T-test p-
319 value ≤ 0.05) (Supplementary file sheet 3). Autoantibody responses in COVID-19 patients were
320 increased for forty proteins, while decreased for seventeen proteins (Figure 2A). The most elevated
321 autoantibody responses in COVID-19 patients were against ATF4 (effect size (beta) = 3.32 SD;
322 T-test p-value ≤ 0.001) and the sperm protein associated with the nucleus on the X chromosome
323 N4 (SPANXN4) (effect size (beta) = 3.32 SD; T-test p-value ≤ 0.001). The latter is also known as
324 spermiogenesis-related protein and belongs to the family of cancer/testis-associated proteins
325 (CTAs)³⁰.

326 We then conducted an analysis using binarized autoimmune response, assuming that all samples
327 with an autoimmune response that exceeds the mean by one s.d. as positive and all others as
328 negative (Supplementary file sheet 4). Using Fisher's exact test, we found twenty-five COVID-19
329 patients had higher RFU values for SPANXN4 compared to only five in controls (Fisher's test p-
330 value ≤ 0.0001) (Figure 2B). Autoantibodies against ATF4, recombining signal binding protein J
331 (RBPJ), and programmed cell death 5 (PDCD5) were also significantly elevated (Fisher's test p-
332 value ≤ 0.05) in the COVID-19 patients. Only the binarized SPANXN4 association reaches the
333 most stringent Bonferroni significance level, that is $p < 0.05 / \text{number of proteins} = 1,318$. In the
334 control group EAPP, SSNA1, and LDHB proteins showed higher autoantibody responses than the
335 cases.

336 **Autoantibody response in the Disc Follow-up cohort confirmed high levels against**
337 **SPANXN4 and other proteins in COVID-19 patients**

338 Following the initial blood sample collection at the time of ICU admission, follow-up samples
339 were collected from fifteen patients at six weeks after recovery from COVID-19. For several
340 proteins, a strong correlation (Pearson's $r^2 \geq 0.69$) was observed between the autoantibody
341 responses at the two sampling time points (Figure 3A). Autoantibody responses against several
342 proteins, including SPANXN4, STK25, TRAF3IP1, AMOTL2, PSMD4, and PPP1R2P9 remained
343 highly elevated ($p \leq 0.05$) at 6 weeks post-recovery follow-up. Particularly, autoantibody
344 responses against SPANXN4 (Figure 3B) stayed elevated at both initial (T1) and follow-up (T2)

345 time points. These observations reveal that SPANXN4 autoantibody responses remain elevated for
346 extended periods, suggesting potential association with chronic health issues.

347 **Relative autoantibody response in the Rep cohort confirms the trend in the Disc cohort**

348 Autoantibody response for the Rep cohort ($n = 48$) was compared with the non-COVID-19 ICU
349 control patients ($N = 28$) (Figure 4A). Autoantibody responses of twenty-six proteins altered
350 significantly (T-test p -value ≤ 0.05) in the Rep cohort. Based on T-test analysis, the most elevated
351 autoantibody response in Rep COVID-19 cohort was found for PRKD2 and BACH1 proteins,
352 which are known for their roles in male reproductive tract development (PRKD2)³¹ and
353 spermatogenesis (BACH1)³². Autoantibody response for SPANXN4 was also higher (effect size
354 (β) = 1.61) in the Rep COVID-19 patients, albeit p -value was slightly higher than 0.05.
355 However, Fisher's exact test indicated that autoantibody response to SPANXN4 remained the
356 highest (Fisher's test p -value = 0.0036) (Figure 4B). At sigma 1, fifteen COVID-19 patients had
357 higher RFU values for SPANXN4 compared to only one in controls. SPANXN4 can therefore be
358 considered fully replicated under the highest standards of a discovery-replication design.
359 PDCD2L, PRKD2, and STK25 showed also higher autoantibody responses in COVID-19 patients
360 (Fisher's test p -value ≤ 0.05).

361 **Analysis of combined cohorts supports that SPANXN4 and STK25 are significantly elevated
362 in COVID-19 patients independent of sampling matrix or patients ethnicity**

363 Principal components analysis (PCA) of protein RFU data from the two cohorts demonstrated
364 strong overlap between COVID-19 samples and the two cohorts did not separate into discrete
365 clusters (Figure 5). Pearson's correlation analysis revealed that the autoantibody responses of the
366 two cohorts have high correlation ($r^2 = 0.73$).

367 At third stage, we combine data from both the Disc and Rep cohorts ($n = 97$) and compared them
368 with combined controls ($n = 76$). Case vs. control analysis revealed that autoantibody responses
369 against fifty-six proteins were significantly altered: 35 autoantibodies with increased and 21
370 autoantibodies with decreased responses (T-test $p \leq 0.05$) (Figure 6A). SPANXN4, ATF4, STK25,
371 and PRKD2 were the proteins with the highest effect size (β). In total forty patients had
372 SPANXN4 RFU higher than 1 sigma value (Fisher's exact test p -value ≤ 0.0001) in the combined
373 COVID-19 cohorts compared with the six patients only in controls (Figure 6B).

374 Furthermore, the autoantibody responses, expressed as RFU z-score for fifty-six proteins that
375 differed significantly between the study groups are shown in Figure 7A. The heatmap shows that
376 most of the proteins display similar pattern of autoantibody ratios across the study cohorts. These
377 analyses demonstrate that our autoantibody response data are highly reproducible despite
378 differences in population ethnicity, different laboratories, and sampling materials (serum vs.
379 plasma in Disc vs. Rep cohorts, respectively).

380 **Protein pathways analysis uncovered up-regulated immune pathways in COVID-19 patients**

381 KEGG and WIKI pathways analysis was performed to identify the functional contribution of
382 autoantibodies targeted proteins in cellular processes and immune-inflammatory systems.
383 Pathways associated with T helper cells (Th1, Th2, and Th17) differentiation, bacterial/viral
384 infections, stress hormones release, and prostate cancer were upregulated in COVID-19 patients
385 (Figure 7B). WIKI pathways were also activated for host immunity and interferon signaling,
386 including T cell activation for SARS-CoV-2 and *Staphylococcus aureus* infections (Figure 7B).

387 **SPANXN4 and STK25 share sequence identity with SPANX- and STK-family proteins but
388 showed unique AB-titers in COVID-19 patients**

389 In order to check cross-reactivities, sequence homology and antigen specificity analysis were
390 performed for SPANXN4 and STK25 against human and viral protein databases. Only few
391 proteins appeared to have more than 50% sequence identity with our target proteins ((SPANXN4
392 with SPANXN1, 2, 3, and 5) and (STK25 with STK 3, 4, 24, and 26)) (Figure 8 and 9). However,
393 many of these homologous proteins were also part of our KREX immunome panel but did not
394 show any significant changes, which means that the observed RFUs are highly specific against the
395 targeted proteins.

396

397 **Discussion**

398 In the current COVID-19 pandemic, there is increasing interest globally in understanding the
399 underlying immunology of COVID-19, as well as revealing new health issues arising from
400 COVID-19 complications. Several papers have described the existence and cross-reactivity of
401 SARS-CoV-2 specific T-cell responses^{33, 34, 35, 36}, as well as correlations with male reproductive
402 system and infertility^{4, 37}. The present study identified and validated several autoantibody
403 responses by screening two independent cohorts of COVID-19 patients with the KREX
404 immunome protein array. The proteins identified with higher autoantibody responses serve
405 important physiological functions and are strongly associated with various immunological and
406 pathological parameters associated with COVID-19 disease.

407 The KREX immunome array contains proteins involved in physiological processes such as MAPK
408 signaling, metabolism, transcription, cell cycle, immunity, and cancer-related pathways. Few of
409 the proteins with the highest mean autoantibody response in COVID-19 patients were RBPJ,
410 TPM1, TACC1, KRT19, and PTPN20. These proteins perform a variety of physiological functions
411 in the human body, with many of them being structural proteins involved in tissue damage and
412 repair mechanisms³⁸. The presence of a high autoantibody response to these proteins suggests that
413 they are overproduced during a pathological condition, such as cancer or a cardiovascular
414 complication^{39, 40}. For example, notch signaling protein RBPJ has been associated with COVID-19
415 pathophysiology and cardiovascular complication⁴¹. Similarly, keratin family proteins (KRT19
416 and KRT15) that are responsible for epithelial cell structural integrity are linked to COVID-19
417 pathogenesis and disease severity⁴². Furthermore, many of these proteins are also involved in male

418 reproductive system physiology and fertility, yet there has been no previous report in COVID-19
419 patients.

420 Our Disc cohort reported higher autoantibodies against SPANXN4, ATF4, RBPJ, and PDCD5
421 proteins compared to the controls. Comparison between COVID-19 baseline (T1) vs. follow-up
422 (T2) samples indicated that SPANXN4 autoantibodies remained elevated at post-recovery stage.
423 Prolonged autoantibody responses may highlight COVID-19 post-acute sequelae by stimulating
424 the humoral immune response in a way that leads to long-term autoantibody production⁴³. The
425 diverse variety of proteins linked to a prolonged autoantibody response suggest that SARS-CoV-
426 2 may stimulate autoantibody formation by molecular mimicry⁴⁴, targeting cardiolipin,
427 cardiolipin-binding proteins, platelet factor 4, prothrombin, and coagulation factors, suggesting
428 their role in coagulopathies, chronic comorbidities and post-infection recovery^{45, 46, 47}. We
429 hypothesize that elevated autoimmune antibodies against SPANXN4, STK25, TRAF3IP1,
430 AMOTL2, PSMD4, and PPP1R2P9 might suggest a similar role. However, Dotan et al.⁴⁸
431 investigated *in-silico* sequence homology of all human proteins with the virus but could not find
432 evidence that any of the proteins mentioned here are part of such a mimicry process. Vice versa,
433 we cannot exclude that the titers might be elevated before the exposure to SARS-CoV-2, due to
434 pre-existing diseases such as cancer or prolonged inflammation.

435 In contrast, the Rep cohort had higher levels of autoantibody responses to SPANXN4, PDCD2L,
436 PRKD2, and STK25 proteins than the controls. Except for SPANXN4, all other proteins with the
437 high autoantibody response were not significantly elevated between the two cohorts but often
438 showed similar trends. These differences could be attributed to the fact that the control group in
439 the Disc cohort was comprised of healthy volunteers, whereas the control group in the Rep study
440 was comprised of ICU patients suffering from bacterial or viral ARDS, or pneumonia.

441 When all COVID-19 patients (N = 97) from both cohorts were merged and compared to all controls
442 (N = 76) from both cohorts, the most significant autoantibody responses were observed against
443 SPANXN4, ATF4, STK25, and PRKD2. ATF4 regulates metabolic and redox processes in the
444 human body, and an increased ATF4 response has been observed in previous coronavirus disease^{49,}
445 ⁵⁰. Fischer et al.¹⁸ suggested that ATF4 also plays role in differentiation of the vas deferens lamina
446 propria layer that helps improve spermatozoa fertilization rate. STK25 and PRKD2 are two
447 important kinases with several physiological roles in our body. However, their role in male
448 reproductive tract physiology is least discussed. A few studies highlight STK25 as androgenic
449 kinase^{16, 17} and PRKD2 role in male reproductive tract development¹⁹.

450 SPANXN4 belongs to a protein family called “sperm protein associated with nucleus in the X
451 chromosome” (SPANX) that are essential for motility and fertilization capacity of male-ejaculated
452 spermatozoa¹⁵. SPANXNs are also known as cancer testis antigens (CTAs) because of their
453 overexpression in tumor tissues, in addition to their normal physiological role in the testis and
454 spermatozoa of healthy males⁵¹. SPANX proteins are expressed in various regions of sperms, and

455 research has shown that the protein family has relevance to male fertility. Particularly, the presence
456 of ACE2 receptors in testicular tissues suggests that SARS-CoV-2 influences male fertility, but
457 the pathogenesis is not clear. No previous COVID-19 study has mentioned SPANXN4
458 involvement in male infertility, neither the pathogenesis is explained. Therefore, the autoantibody
459 response measured in the current study may suggest a novel diagnostic and treatment marker for
460 male fertility. Previously, one hepatitis C virus study has shown that SPANXN4 interacts with the
461 virus, potentially increases virus infectivity, albeit no reproductive performance was discussed⁵².
462 Increased levels of autoantibodies against testis-related proteins suggest their role in affecting male
463 reproductive system, and thus declining male fertility in COVID-19. Although several
464 investigations have found that COVID-19 patients have altered seminal parameters and decreased
465 reproductive hormone levels⁵³, histological or functional abnormalities in male genital system⁵⁴,
466 damaged blood-testis barrier⁵⁵, and impaired spermatogenesis⁵⁶, the cause of this comorbidity has
467 not yet been investigated, and remains unknown.

468 Despite their ethnic diversity, which included Middle Eastern, Africans, Caucasians, Asians, and
469 South Asians populations, correlation analysis, hierarchical, and PCA clustering demonstrated that
470 both cohorts shared similarities in autoantibody responses. Therefore, strong correlation ($r^2 = 0.73$)
471 between these cohorts demonstrate that autoantibody response data of COVID-19 patients are
472 highly reproducible among different ethnic populations. These findings are consistent with our
473 prior COVID-19 proteomics study that looked at immune-inflammatory markers in five different
474 demographic cohorts (manuscript accepted).

475 Several previous COVID-19 studies have reported elevated immune-inflammatory responses,
476 including cytokine-storm in COVID-19 patients. Perhaps, we observed relatively elevated albeit
477 non-significant autoantibody responses to immune cytokines like IL1A and IL1B proteins. KEGG
478 and WIKI pathways analysis showed that autoantibody responses to immune proteins activated T
479 cell responses against infection and T helper cell differentiation. Li et al.,⁵⁷ observed that Th17
480 differentiation and cytokine response pathways play a key role in pathogenesis of COVID-19 and
481 autoimmune diseases. Pathways analysis suggests that many immune cell responses specific to
482 SARS-CoV-2 or bacterial infections may precede chronic inflammatory disorders and the
483 respiratory failure⁵⁸. Furthermore, an abnormal T helper cell response, combined with overactive
484 interferon signaling, promote the differentiation of B cells, which produce autoantibodies and
485 cause autoimmune diseases⁵⁹.

486 In conclusion, these findings reveal unique autoantibody response against several proteins that
487 play diverse though important function in COVID-19 complications. These observations also
488 highlight the importance of the humoral immune response, as well as numerous other previously
489 unknown immunological pathways in COVID-19 pathogenesis. Particularly, elevated levels of
490 autoantibodies against the testicular tissue specific protein SPANXN4 in both cohorts offer
491 significant evidence of anticipating the protein's role in COVID-19 associated male reproductive
492 complications. Overall, these finding not only revalidate autoantibody responses against
493 SPANXN4 in COVID-19 but also predict novel pathological associations that may contribute to
494 COVID-19 post-recovery comorbidities. SPANXN family proteins are known as CTAs⁶⁰ that play

495 essential role in spermatogenesis, however, their role in male fertility in the COVID-19 patients is
496 previously unknown.

497 **Author Contributions:**

498 F.S., H.B.A. and O.M.E. designed, conceived, and led the study. M.A.Y.A., V.M.A., and A.M. led
499 the Disc Cohort sample collection, processing, and ethical approvals. H.B.A. and N.V. optimized
500 the assays on Disc Cohort. I.B. and H.B.A. run the assays on Disc samples. K.S. and M.U.S.
501 performed statistics. E.J.S., D.P., H.S., and A.M.K.C. organized and collected samples for Rep
502 Cohort. T-M.T., P.E.M., and J.M.B. run the assays on Rep samples J.B. and F.M. performed
503 annotation and treemap analyses. K.S., F.S., F.M., M.U.S., H.B.A., O.M.E., J.D., J.B., and A.A.
504 interpreted the data. M.U.S., K.S., H.B.A., and F.S. wrote the manuscript. All authors reviewed
505 the manuscript and have read and agreed to the published version of the manuscript.

506 **Funding:** Research conducted on Qatar cohort was funded by project funding from Infectious
507 Diseases Interdisciplinary Research Program (ID-IDRP) at QBRI and a grant fund from Hamad
508 Medical Corporation (fund number MRC-05-003).

509 **Institutional Review Board Statement:** The study on Qatar Cohort was conducted according to
510 the Ministry of Public Health (MOPH) guidelines and approved by the Institutional Review Board
511 Research Ethics Committee of the Hamad Medical Corporation (reference MRC-05-003).

512 **Acknowledgments:** We would like to thank all the patients, volunteers, and healthcare co-workers
513 from HMC and NYP/WCMC hospitals, and Rudolph Engelke for providing the R-code for
514 functional enrichment. We also acknowledge the help provided by the Anti-Doping Lab-Qatar
515 (ADLQ) and Qatar Red Crescent (QRC) for recruiting control individuals. The Qatar cohort
516 research was supported by the Proteomics core facility and ID-IDRP project at QBRI. This work
517 was also strongly supported by the Biomedical Research Program at Weill Cornell Medicine in
518 Qatar, a program funded by the Qatar Foundation.

519 **Conflicts of Interest:** There is no conflict of interest.

520
521

522 **References**

523

524 1. Chen G, *et al.* Clinical and immunological features of severe and moderate coronavirus
525 disease 2019. *J Clin Invest* **130**, 2620-2629 (2020).

526

527 2. Pfortmueller CA, Spinetti T, Urman RD, Luedi MM, Schefold JC. COVID-19-associated
528 acute respiratory distress syndrome (ARDS): Current knowledge on pathophysiology
529 and ICU treatment – A narrative review. *Best Practice & Research Clinical
530 Anaesthesiology*, (2020).

531

532 3. Ashraf UM, *et al.* SARS-CoV-2, ACE2 expression, and systemic organ invasion.
533 *Physiological Genomics* **53**, 51-60 (2021).

534

535 4. Sun J. The hypothesis that SARS-CoV-2 affects male reproductive ability by regulating
536 autophagy. *Med Hypotheses* **143**, 110083 (2020).

537

538 5. Chang SE, *et al.* New-onset IgG autoantibodies in hospitalized patients with COVID-19.
539 *Nature Communications* **12**, 5417 (2021).

540

541 6. Bastard P, *et al.* Autoantibodies against type I IFNs in patients with life-threatening
542 COVID-19. *Science* **370**, (2020).

543

544 7. Garcia-Beltran WF, *et al.* COVID-19-neutralizing antibodies predict disease severity and
545 survival. *Cell* **184**, 476-488.e411 (2021).

546

547 8. Wang EY, *et al.* Diverse functional autoantibodies in patients with COVID-19. *Nature*
548 **595**, 283-288 (2021).

549

550 9. Woodruff MC, Ramonell RP, Lee FE-H, Sanz I. Clinically identifiable autoreactivity is
551 common in severe SARS-CoV-2 Infection. *medRxiv*, 2020.2010.2021.20216192 (2020).

552

553 10. Woodruff MC, *et al.* Extrafollicular B cell responses correlate with neutralizing
554 antibodies and morbidity in COVID-19. *Nature Immunology* **21**, 1506-1516 (2020).

555

556 11. Zuo Y, *et al.* Prothrombotic autoantibodies in serum from patients hospitalized with
557 COVID-19. *Science Translational Medicine* **12**, eabd3876 (2020).

558

559 12. Tay MZ, Poh CM, Rénia L, MacAry PA, Ng LFP. The trinity of COVID-19: immunity,
560 inflammation and intervention. *Nature Reviews Immunology* **20**, 363-374 (2020).

561

562 13. Applications of Functional Protein Arrays for Detection and Development of
563 Autoantibody-based Diagnostics and Therapeutics.) (2018).

564

565 14. Fritzler MJ, Martinez-Prat L, Choi MY, Mahler M. The Utilization of Autoantibodies in
566 Approaches to Precision Health. *Frontiers in Immunology* **9**, (2018).

567

568 15. Urizar-Arenaza I, *et al.* SPANX-A/D protein subfamily plays a key role in nuclear
569 organisation, metabolism and flagellar motility of human spermatozoa. *Scientific
570 Reports* **10**, 5625 (2020).

571

572 16. Gill-Sharma MK. Testosterone Retention Mechanism in Sertoli Cells: A Biochemical
573 Perspective. *Open Biochem J* **12**, 103-112 (2018).

574

575 17. Hammes A, *et al.* Role of Endocytosis in Cellular Uptake of Sex Steroids. *Cell* **122**, 751-
576 762 (2005).

577

578 18. Fischer C, *et al.* Activating transcription factor 4 is required for the differentiation of the
579 lamina propria layer of the vas deferens. *Biol Reprod* **70**, 371-378 (2004).

580

581 19. Dai D-H, *et al.* Exploration of miRNA and mRNA Profiles in Fresh and Frozen-Thawed
582 Boar Sperm by Transcriptome and Small RNA Sequencing. *International Journal of
583 Molecular Sciences* **20**, 802 (2019).

584

585 20. Razavi SM, Sabbaghian M, Jalili M, Divsalar A, Wolkenhauer O, Salehzadeh-Yazdi A.
586 Comprehensive functional enrichment analysis of male infertility. *Scientific reports* **7**,
587 15778-15778 (2017).

588

589 21. Organization WH. Clinical management of severe acute respiratory infection when novel
590 coronavirus (nCoV) infection is suspected: interim guidance, 25 January 2020.). World
591 Health Organization (2020).

592

593 22. Su C, *et al.* Identifying organ dysfunction trajectory-based subphenotypes in critically ill
594 patients with COVID-19. *medRxiv*, 2020.2007.2016.20155382 (2020).

595

596 23. Finkelsztein EJ, *et al.* Comparison of qSOFA and SIRS for predicting adverse outcomes of
597 patients with suspicion of sepsis outside the intensive care unit. *Crit Care* **21**, 73 (2017).

598

599 24. Schenck EJ, *et al.* Circulating cell death biomarker TRAIL is associated with increased
600 organ dysfunction in sepsis. *JCI Insight* **4**, (2019).

601

602 25. Adeola HA, Smith M, Kaestner L, Blackburn JM, Zerbini LF. Novel potential serological
603 prostate cancer biomarkers using CT100+ cancer antigen microarray platform in a multi-
604 cultural South African cohort. *Oncotarget* **7**, 13945-13964 (2016).

605

606 26. Blackburn JM, Shoko A, Beeton-Kempen N. Miniaturized, microarray-based assays for
607 chemical proteomic studies of protein function. *Methods Mol Biol* **800**, 133-162 (2012).

608

609 27. Da Gama Duarte J, Goosen RW, Lawry PJ, Blackburn JM. PMA: Protein Microarray
610 Analyser, a user-friendly tool for data processing and normalization. *BMC research notes*
611 **11**, 156 (2018).

612

613 28. Bernhardt J, Funke S, Hecker M, Siebourg J. Visualizing Gene Expression Data via
614 Voronoi Treemaps. In: *2009 Sixth International Symposium on Voronoi Diagrams*)
615 (2009).

616

617 29. Blackburn J, *et al.* Quantitative, Epitope-specific, Serological Screening of COVID-19
618 Patients Using a Novel Multiplexed Array-based Immunoassay Platform. *medRxiv*,
619 2020.2009.2025.20201269 (2020).

620

621 30. Kouprina N, *et al.* The SPANX gene family of cancer/testis-specific antigens: rapid
622 evolution and amplification in African great apes and hominids. *Proc Natl Acad Sci U S A*
623 **101**, 3077-3082 (2004).

624

625 31. Nie X, Arend LJ. Novel roles of Pkd2 in male reproductive system development.
626 *Differentiation* **87**, 161-171 (2014).

627

628 32. Yu B, *et al.* Cigarette Smoking Is Associated with Human Semen Quality in Synergy with
629 Functional NRF2 Polymorphisms1. *Biology of Reproduction* **89**, (2013).

630

631 33. Grifoni A, *et al.* Targets of T Cell Responses to SARS-CoV-2 Coronavirus in Humans with
632 COVID-19 Disease and Unexposed Individuals. *Cell* **181**, 1489-1501.e1415 (2020).

633

634 34. Peng Y, *et al.* Broad and strong memory CD4(+) and CD8(+) T cells induced by SARS-CoV-
635 2 in UK convalescent individuals following COVID-19. *Nat Immunol* **21**, 1336-1345
636 (2020).

637

638 35. Reynolds CJ, *et al.* Discordant neutralizing antibody and T cell responses in
639 asymptomatic and mild SARS-CoV-2 infection. *Sci Immunol* **5**, (2020).

640

641 36. Sekine T, *et al.* Robust T Cell Immunity in Convalescent Individuals with Asymptomatic or
642 Mild COVID-19. *Cell* **183**, 158-168.e114 (2020).

643

644 37. Delle Fave RF, Polisini G, Giglioni G, Parlavecchio A, Dell'Atti L, Galosi AB. COVID-19 and
645 male fertility: Taking stock of one year after the outbreak began. *Arch Ital Urol Androl*
646 **93**, 115-119 (2021).

647

648 38. Zhang X, Yin M, Zhang L-J. Keratin 6, 16 and 17-Critical Barrier Alarmin Molecules in Skin
649 Wounds and Psoriasis. *Cells* **8**, 807 (2019).

650

651 39. Lv Q, Shen R, Wang J. RBPJ inhibition impairs the growth of lung cancer. *Tumour Biol* **36**,
652 3751-3756 (2015).

653

654 40. Saha SK, *et al.* KRT19 directly interacts with β -catenin/RAC1 complex to regulate NUMB-dependent NOTCH signaling pathway and breast cancer properties. *Oncogene* **36**, 332-349 (2017).

655

656

657

658 41. Breikaa RM, Lilly B. The Notch Pathway: A Link Between COVID-19 Pathophysiology and Its Cardiovascular Complications. *Front Cardiovasc Med* **8**, 681948-681948 (2021).

659

660

661 42. Gisby J, *et al.* Longitudinal proteomic profiling of dialysis patients with COVID-19 reveals markers of severity and predictors of death. *Elife* **10**, e64827 (2021).

662

663

664 43. Proal AD, VanElzakker MB. Long COVID or Post-acute Sequelae of COVID-19 (PASC): An Overview of Biological Factors That May Contribute to Persistent Symptoms. *Frontiers in Microbiology* **12**, (2021).

665

666

667

668 44. Liu Y, Sawalha AH, Lu Q. COVID-19 and autoimmune diseases. *Curr Opin Rheumatol* **33**, 155-162 (2021).

669

670

671 45. Leng L, *et al.* Potential microenvironment of SARS-CoV-2 infection in airway epithelial cells revealed by Human Protein Atlas database analysis. *bioRxiv*, 2020.2004.2016.045799 (2020).

672

673

674

675 46. Mishra A, Chanchal S, Ashraf MZ. Host-Viral Interactions Revealed among Shared Transcriptomics Signatures of ARDS and Thrombosis: A Clue into COVID-19 Pathogenesis. *TH Open* **4**, e403-e412 (2020).

676

677

678

679 47. Root-Bernstein R. COVID-19 coagulopathies: Human blood proteins mimic SARS-CoV-2 virus, vaccine proteins and bacterial co-infections inducing autoimmunity. *BioEssays* **n/a**, 2100158.

680

681

682

683 48. Dotan A, Muller S, Kanduc D, David P, Halpert G, Shoenfeld Y. The SARS-CoV-2 as an instrumental trigger of autoimmunity. *Autoimmun Rev* **20**, 102792 (2021).

684

685

686 49. Kötitz J, *et al.* Oxygen-dependent ATF-4 stability is mediated by the PHD3 oxygen sensor. *Blood* **110**, 3610-3617 (2007).

687

688

689 50. Liao Y, Fung TS, Huang M, Fang SG, Zhong Y, Liu DX. Upregulation of CHOP/GADD153 during coronavirus infectious bronchitis virus infection modulates apoptosis by restricting activation of the extracellular signal-regulated kinase pathway. *Journal of virology* **87**, 8124-8134 (2013).

690

691

692

693

694 51. Zendman AJ, *et al.* The human SPANX multigene family: genomic organization, alignment and expression in male germ cells and tumor cell lines. *Gene* **309**, 125-133 (2003).

695

696

697

698 52. Ngo HTT, Pham LV, Kim J-W, Lim Y-S, Hwang SB. Modulation of mitogen-activated
699 protein kinase-activated protein kinase 3 by hepatitis C virus core protein. *Journal of*
700 *virology* **87**, 5718-5731 (2013).

701

702 53. Khalili MA, *et al.* Male Fertility and the COVID-19 Pandemic: Systematic Review of the
703 Literature. *World J Mens Health* **38**, 506-520 (2020).

704

705 54. Youssef K, Abdelhak K. Male genital damage in COVID-19 patients: Are available data
706 relevant? *Asian J Urol*, (2020).

707

708 55. Peirouvi T, *et al.* COVID-19 disrupts the blood-testis barrier through the induction of
709 inflammatory cytokines and disruption of junctional proteins. *Inflamm Res* **70**, 1165-
710 1175 (2021).

711

712 56. Li H, *et al.* Impaired spermatogenesis in COVID-19 patients. *EClinicalMedicine* **28**,
713 100604 (2020).

714

715 57. Li Z, *et al.* Bioinformatic analyses hinted at augmented T helper 17 cell differentiation
716 and cytokine response as the central mechanism of COVID-19-associated Guillain-Barré
717 syndrome. *Cell Proliferation* **54**, e13024 (2021).

718

719 58. Ouyang Y, *et al.* Downregulated Gene Expression Spectrum and Immune Responses
720 Changed During the Disease Progression in Patients With COVID-19. *Clinical Infectious
721 Diseases* **71**, 2052-2060 (2020).

722

723 59. Zhang X-M, Liu C-Y, Shao Z-H. Advances in the role of helper T cells in autoimmune
724 diseases. *Chin Med J (Engl)* **133**, 968-974 (2020).

725

726 60. Chiriva-Internati M, Cobos E, Da Silva DM, Kast WM. Sperm fibrous sheath proteins: a
727 potential new class of target antigens for use in human therapeutic cancer vaccines.
728 *Cancer Immun* **8**, 8 (2008).

729

730

731

732

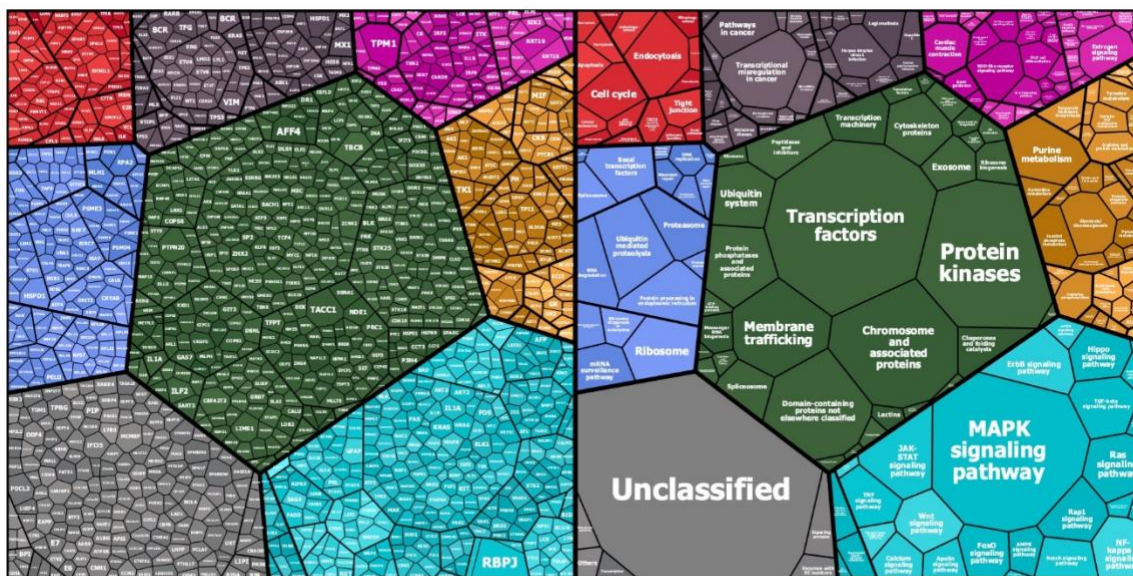
733 **Table 1:** Summary metadata of COVID-19 case and control cohorts

734

Study Specification	Condition	Discovery Cohort (Disc)	Replication Cohort (Rep)
Cohort Size	Control	48	28
	COVID-19	49	48
	COVID-19 Follow-up	15	
Gender (Male, Female)	Control	46 M + 2 F	19 M + 9 F
	COVID-19	48 M + 1 F	40 M + 8 F
	COVID-19 Follow-up	15 M	
Age (IQR)	Control	38 (9)	66 (26)
	COVID-19	47 (20)	57 (22)
	COVID-19 Follow-up	49 (11)	
BMI (mean (IQR))	Control	25.3 (9.2)	25.9 (9.4)
	COVID-19	29.9 (6.2)	28.9 (7.3)
	COVID-19 Follow-up	28.7 (6.4)	
Sampling Time (media days (IQR))	COVID-19	5 (3) days after ICU admission	6 (6) days after ICU admission
	COVID-19 Follow-up	Six weeks after recovery	
Status Controls	Healthy	ICU Bacterial ARDS & Pneumonia, ICU H1N1 ARDS & Pneumonia	
Status COVID-19	Severe	Severe, ARDS, Pneumonia	
Hospital	ICU, HMC, Qatar	ICU, New York, USA	
Ethnicity (%)	South Asian (69), Middle East and North Africa (MENA) (25). Other (6)	White (31), Asian (10), African (9), Other/Unspecified (50)	
Matrix, Tubes, and Virus Inactivation	Serum, non-EDTA coated, viral inactivation using 10% Triton X100	Plasma, EDTA coated, viral inactivation using 10% Triton X100	

735

736 Figure 1: Mapping of KREX Array proteins to KEGG categories (KEGG Pathway and KEGG
737 Brite): Protein symbols and median fluorescent antibody signals (treemap cell size) are represented
738 according their KEGG category assignment (www.kegg.jp; accessed on 14.Nov.2021). The other
739 main categories are defined as cellular processes (top left - red), Human diseases (top middle -
740 greyish purple), Organismal systems (to right - magenta), Genetic information processing (left -
741 blue), Brite protein families (center - dark green), metabolism (right - orange), environmental
742 information processing (bottom right - cyan). Unmapped proteins are considered as "Not included
743 in Pathway or Brite" (bottom left - grey).

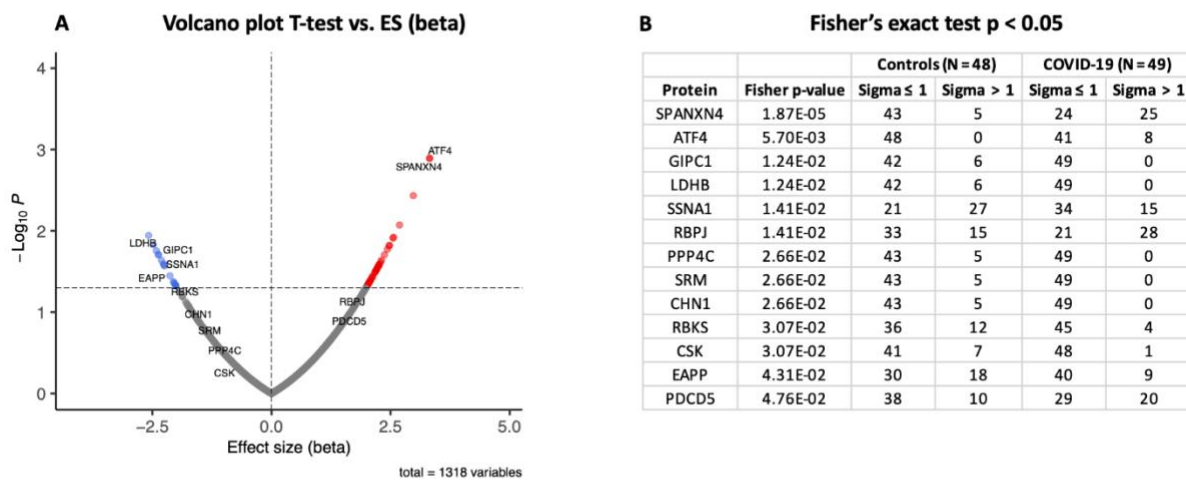


744
745
746

747 Figure 2: Differential protein autoantibody response analysis of COVID-19 Discovery cohort
748 performed using T-test (A) and Fisher's exact test (B). A) Volcano graph of 1,318 proteins
749 compares COVID-19 case (n = 49) vs. healthy controls (n = 48). Red dots represent proteins with
750 an elevated autoantibody response, while blue dots represent proteins with a lower autoantibody
751 response in COVID-19 patients. Proteins with Fisher's test p-value ≤ 0.05 are labelled in the
752 volcano graph. B) Table on Fisher's exact statistics comparing subjects (numbers) of COVID-19
753 (n = 49) and the control (n = 48) groups for only thirteen proteins that showed significantly altered
754 (p-value ≤ 0.05) autoantibody responses at sigma > 1.

Fig. 2

Discovery Cohort: Case vs. Control - 1318 Protein AB-titers



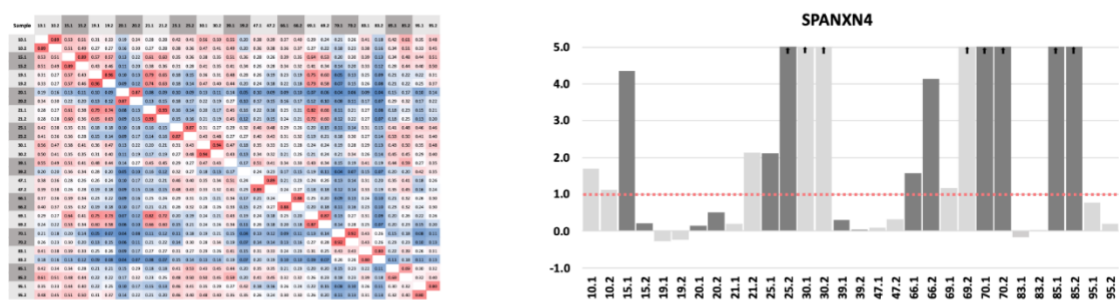
755
756

757 Figure 3: Autoantibody response in the Discovery cohort (T1 = sampling during ICU admission)
758 and follow-up patients (T2 = sampling after recovery). A) Spearman rank correlation analysis of
759 fifteen Discovery cohort samples collected at two different time points show strong correlation (r
760 ≥ 0.69) of autoantibody responses for the proteins. B) The histogram of Discovery cohort samples
761 shows that the z-score RFU of SPANXN4 protein remains elevated in many patients even after
762 COVID-19 recovery.

Fig. 3

Discovery Cohort: Cases – Follow Up

A Pearson correlation plot all AB-titers T1 vs T2 B Z-scored RFU SPANXN4 - T1 & T2

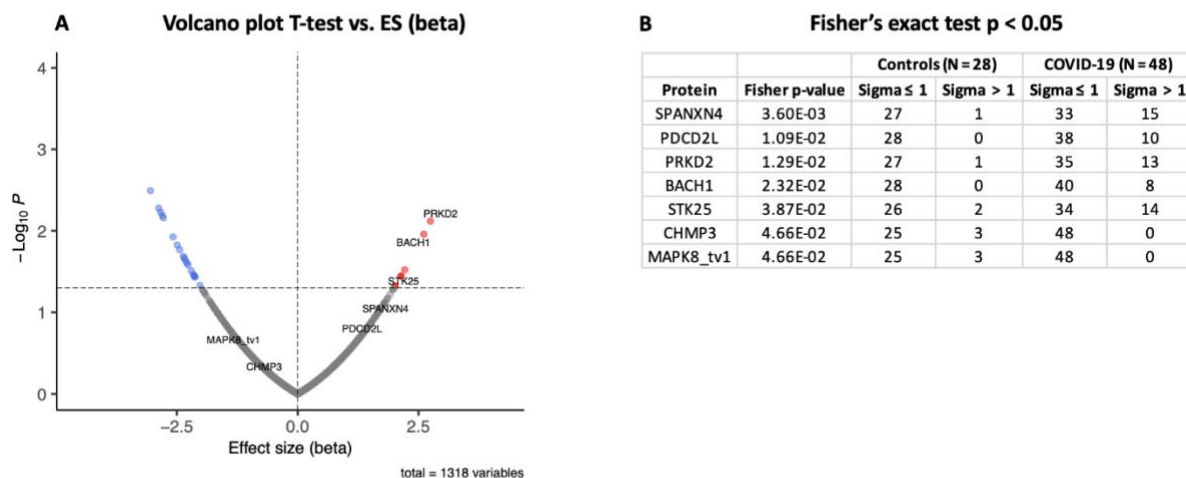


763

764 Figure 4: Differential protein autoantibody response analysis of COVID-19 Replication cohort
765 performed using T-test (A) and Fisher's exact test (B). A) Volcano graph of 1,318 proteins
766 compares COVID-19 cases (n = 48) vs. non-COVID-19 ICU controls (n = 28). Red dots represent
767 proteins with a high autoantibody response, while blue dots represent proteins with a low
768 autoantibody response in COVID-19 positive patients. Only proteins with Fisher's test p-value \leq
769 0.05 are labelled in the volcano graph. B) Table on Fisher's exact statistics comparing subjects
770 (numbers) of COVID-19 (n = 49) and the control (n = 48) groups for only thirteen proteins that
771 showed significantly altered (p-value ≤ 0.05) autoantibody responses at sigma > 1.

Fig. 4

Replication Cohort: Case vs. Control - 1318 Protein AB-titers

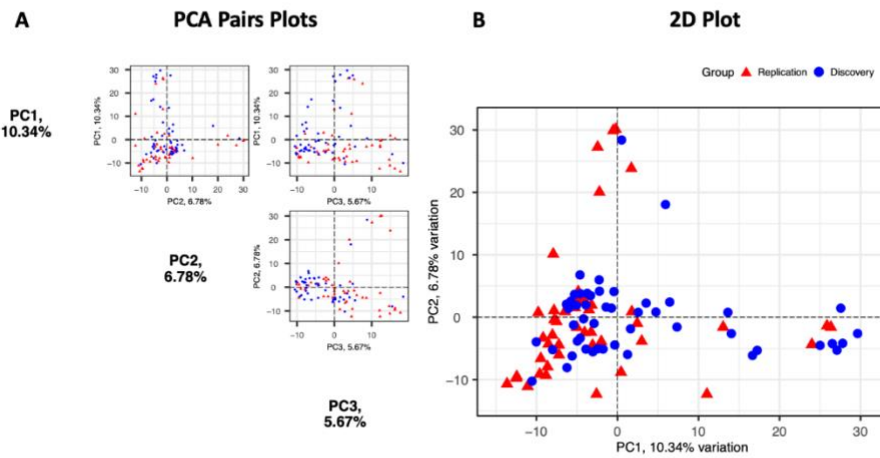


772
773

774 Figure 5: Principal Components Analysis of the Discovery (n = 49, blue circles) and the
775 Replication cohorts (n = 48, red triangles). Each point represents a sample. A) PCA pair plot
776 compares PC1 to PC3. The proportion of variance explained in our cohorts by each PC is shown
777 in parentheses on the axis labels. B) PCA 2D plot with PC1 and PC2, which together describe
778 17.12% diversity between the cohorts.

Fig. 5

Combined Cohorts: Case vs. Control - 1318 Protein AB-titers

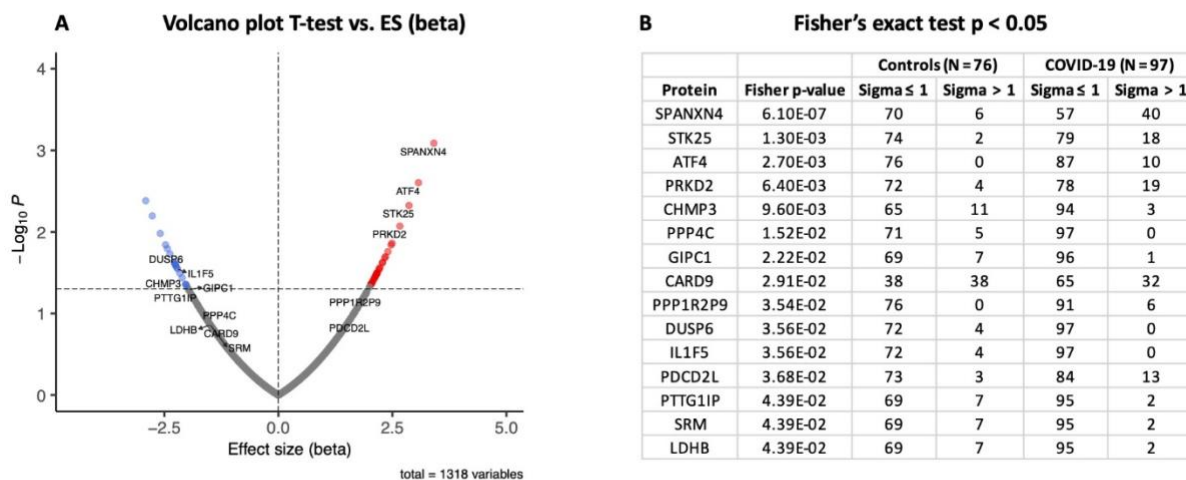


779
780

781 Figure 6: Differential protein autoantibody response analysis of Combined Cohorts performed
782 using T-test (A) and Fisher's exact test (B). A) Volcano graph of 1,318 AB-protein titers compares
783 COVID-19 cases (n = 97) vs. controls (n = 76). Red dots represent proteins with a high
784 autoantibody response, while blue dots represent proteins with a low autoantibody response in
785 COVID-19 positive patients. Only proteins with Fisher's test p-value ≤ 0.05 are labelled in the
786 volcano graph. B) Table on Fisher's exact statistics comparing subjects (numbers) of COVID-19
787 (n = 49) and the control (n = 48) groups for only thirteen proteins that showed significantly altered
788 (p-value ≤ 0.05) autoantibody responses at sigma > 1.

Fig. 6

Combined Cohorts: Case vs. Control - 1318 Protein AB-titers

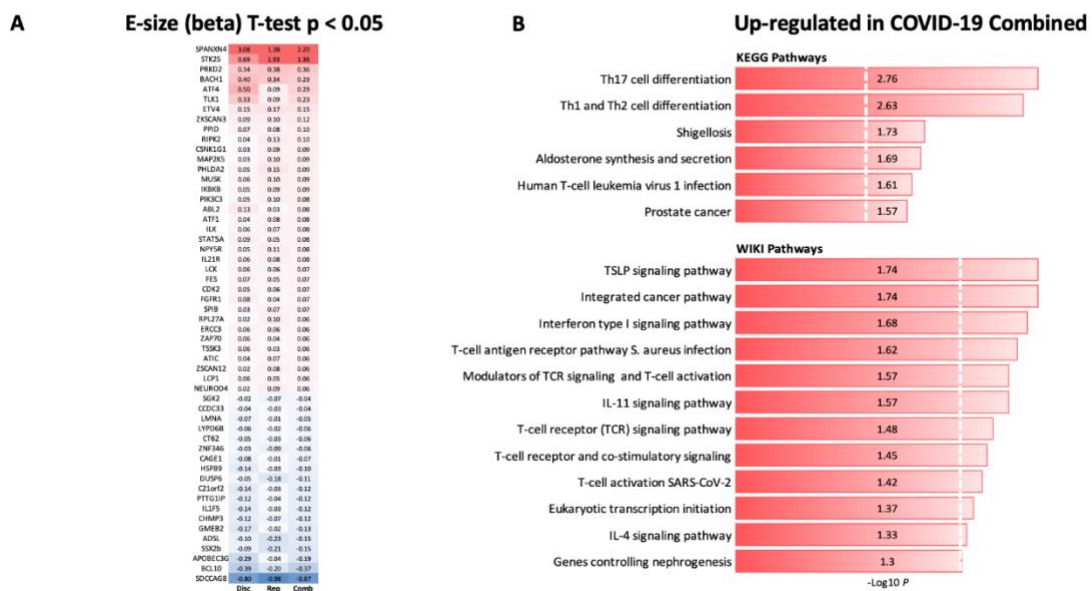


789
790

791 Figure 7: Heatmap of autoantibody response pattern among different cohorts (A) and bar plots for
 792 pathways analysis. A) Heatmap of relative estimates (case vs. control) of autoantibody responses
 793 to fifty-six proteins in the Discovery, Replication, and Combined cohorts. Only proteins with
 794 significantly altered autoantibody responses were selected. Red color indicates higher and blue
 795 color indicates lower autoantibody responses against the proteins. B) KEGG and WIKI pathways
 796 analysis presented as bar-plot shows overactivated pathways in COVID-19 patients. Only
 797 pathways with T-test p-value ≤ 0.05 are presented in the bar-plot.

Fig. 7

Combined Cohorts: Case vs. Control - 1318 Protein AB-titers - Enriched Pathways T-test

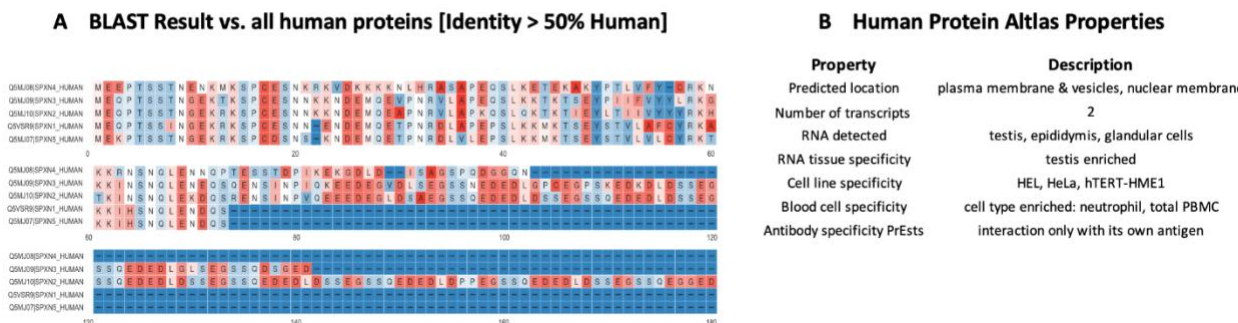


798
 799

800 Figure 8: SPANXN4 protein sequence identity and antigen specificity analysis. A) Sequence
 801 alignment of proteins showing $\geq 50\%$ identity with SPANXN4. B) Summary of properties of
 802 SPANXN4 protein from Human protein atlas. C) Autoantibody responses to SPANXN family
 803 proteins with high sequence identity to SPANXN4 that were part of the KREX immunome panel.

Fig. 8

Overview SPANX4 Properties



C Combined Cohorts: Case vs. Control - SPANX Family AB-titers

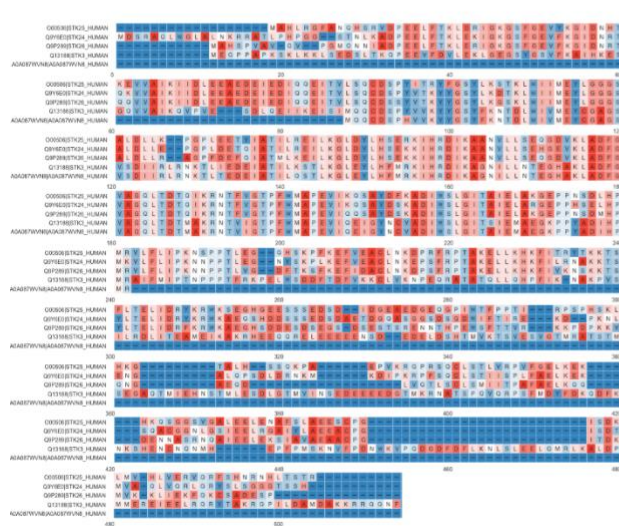
Controls (N = 76) COVID-19 (N = 97)							
Protein	T-test p-value	T-test Ratio	Fisher p-value	Sigma ≤ 1	Sigma > 1	Sigma ≤ 1	Sigma > 1
SPANXN4	8.17E-04	-2.20E+00	6.06E-07	70	6	57	40
SPANXN2	9.53E-01	2.13E-02	5.04E-01	52	24	71	26
SPANXN1	4.28E-01	-3.18E-01	1.00E+00	70	6	90	7

804
 805

806 Figure 9: STK25 protein sequence identity and antigen specificity analysis. A) Sequence alignment
 807 of proteins showing $\geq 50\%$ identity with STK25. B) Summary of properties of STK25 protein
 808 from Human Protein Atlas. C) Autoantibody responses to STK family proteins with high sequence
 809 identity to STK25 that were part of the KREX immunome panel.

Fig. 9

A BLAST Result vs. all human proteins [Identity > 50% Human]



B Human Protein Atlas Properties

Property	Description
Predicted location	intracellular
Number of transcripts	19
RNA detected	all tissues
RNA tissue specificity	skeletal muscles
Cell line specificity	low cell line specificity
Blood cell specificity	detected in all without cell-type specificity

C Combined Cohorts: Case vs. Control - STK Family AB-titers

Protein	T-test p-value	T-test Ratio	Fisher p-value	Controls (N = 76)		COVID-19 (N = 97)	
				Sigma ≤ 1	Sigma > 1	Sigma ≤ 1	Sigma > 1
STK25	4.7E-03	1.36E+00	1.29E-03	74	2	79	18
STK10	8.2E-01	9.91E-03	5.05E-01	76	0	95	2
STK11	2.2E-01	2.83E-02	1.00E+00	76	0	97	0
STK16	3.3E-01	-2.66E-02	1.00E+00	76	0	97	0
STK17B	6.2E-01	1.78E-02	1.00E+00	76	0	96	1
STK24	9.8E-01	7.62E-04	1.00E+00	76	0	97	0
STK26	3.5E-01	4.61E-02	4.68E-01	74	2	91	6
STK3	9.3E-01	4.82E-03	1.00E+00	76	0	97	0
STK32A	7.4E-01	-1.32E-02	1.00E+00	76	0	97	0
STK32C	1.5E-01	-7.63E-02	1.00E+00	75	1	96	1
STK33	6.6E-01	-9.29E-02	1.00E+00	73	3	92	5
STK38	7.9E-01	9.64E-03	1.00E+00	76	0	97	0
STK38L	9.0E-01	4.48E-03	1.00E+00	76	0	97	0
STK4	7.8E-01	9.23E-03	1.00E+00	76	0	97	0